A comprehensive insight in the MOCVD of aluminum through interaction between reactive transport modeling and targeted growth experiments

Theodora C. Xenidou, Nathalie Prud'homme, Constantin Vahlas, Nicholas C. Markatos, Andreas G. Boudouvis

A Comprehensive Insight in the MOCVD of Aluminum Through Interaction Between Reactive Transport Modeling and Targeted Growth Experiments

T. C. Xenidou[a], N. Prud'homme[b], C. Vahlas[b], N. C. Markatos[a], and A. G. Boudouvis[a]

[a] National Technical University of Athens, School of Chemical Engineering, Athens 15780, GREECE
[b] CIRIMAT-CNRS, ENSIACET, 31077 Toulouse cedex 4, FRANCE

Growth experiments and reactive transport modeling were combined to formulate a comprehensive predictive model for aluminum growth from dimethylethylamine alane. The growth-rate profile was experimentally investigated as a function of substrate temperature. The reactive transport model, built under the computational fluid dynamics software PHOENICS, was used to reproduce the experimental measurements and to contribute to the understanding of the aluminum growth process, under sub-atmospheric pressure conditions. The growth mechanism of aluminum films was based on well established in literature reaction order and activation energy of homogeneous and heterogeneous chemical reactions. The reactive transport model was used further to investigate the effect of some key operating parameters on the process output. Simulation results are suggestive of modifications in the operating parameters that could enhance the growth rate and the spatial uniformity of the film thickness.

Introduction

Aluminum (Al) is the major element in complex metallic alloys (CMAs), including quasi-crystalline phases (1). Such phases present strong technological potential for applications on complex-in-shape substrates. Metal-Organic Chemical Vapor Deposition (MOCVD) is a promising technique to meet this challenge and for this reason the growth of Al films was selected as the first important step towards the establishment of a robust, innovative process for the preparation of CMA coatings.

The successful implementation of a MOCVD process in the large-scale production of Al-based intermetallic alloys depends on the ability to determine optimal operating conditions in well-designed reactor configurations. Modeling of the MOCVD process and simulation at appropriately selected experimental conditions is the efficient, alternative route to the time-consuming experimental investigation (2). The preliminary results of the supplementary use of growth experiments and computational fluid dynamics (CFD) simulations concerned the Al growth from dimethylethylamine alane (DMEAA) in the narrow temperature range of 200^{o}C-220^{o}C (3). The selection of DMEAA as the metal-organic precursor for Al was based on the results of previous experimental studies (4-9).

In the present work, the experimental investigation of Al growth in an expanded temperature range, enhance the comprehensive modeling of the MOCVD process. The measured growth-rate profiles of Al films are used to formulate a reactive transport model, pointing out the influence of the substrate temperature. The present model, that is

a more elaborate version of the one reported earlier (3), is used further to investigate the effect of key operating parameters on Al growth rate and its spatial uniformity over the substrate surface.

Experimental

Growth experiments were performed in the experimental setup reported previously (3). This setup is composed of a stagnant flow, cylindrical, stainless steel reactor. Its base pressure is 10^{-6} Torr. The reactor is equipped with a showerhead system above a resistively heated susceptor whose diameter is 58 mm. 99% pure DMEAA was used as received. Two 99.999 % pure nitrogen lines were used: one for bubbling through the Al precursor and one for the dilution of the input gas.

The growth-rate profile of Al films on silicon substrates was measured as a function of substrate temperature, in the range 160°C-260°C. The experimental growth rate was calculated as the thickness divided by the deposition time, which was taken equal to the duration of each experiment, i.e. 120 min. Experimental conditions and measured growth rates are summarized in Table I. The measurements indicate that the growth rate increases as the substrate temperature increases up to 200°C and then decreases with further increase of temperature above 200°C.

TABLE I. Experimental Operating Conditions and Measured Growth Rates.

Sample name	N_2 dilution flow rate (sccm)	N_2 carrier flow rate (sccm)	DMEAA bubbler temperature (°C)	Inlet gas temperature (°C)	Wall temperature (°C)	Reactor pressure (Torr)	Substrate temperature (°C)	Average growth rate (Å/min)
Exp1	305	25	9	65	25	10	160	161,6
Exp2	305	25	9	65	25	10	200	237,8
Exp3	305	25	9	65	25	10	220	227,2
Exp4	305	25	9	65	25	10	260	79,0

Reactive Transport Model

The phenomena involved in MOCVD processes include coupled fluid flow, heat transfer, mass transport of multiple gas species and chemical reactions in the gas phase and on the heated substrates. The coupled partial differential equations for the conservation of total mass, momentum, energy and individual species were used to formulate a mathematical model for Al growth process. All these differential equations can be cast in the following general form (10):

$$\nabla \cdot \left(\rho \vec{V} \phi - \Gamma_\phi \nabla \phi \right) = S_\phi \qquad [1]$$

In Eq. [1], ρ is the density, $\vec{V}$ is the velocity vector, Γ_ϕ is the effective exchange coefficient of variable ϕ and S_ϕ is the source term expressing the production of ϕ inside the domain of interest. The CFD code PHOENICS (11) was used to simultaneously solve the partial differential equations with the appropriate boundary conditions (12). Detailed discussion of the assumptions made and the boundary conditions used can be found in the preliminary simulation of the MOCVD reactor (3).

While the axial symmetry of the vertical MOCVD reactor calls for two-dimensional (2D) approximation of the reactor, the non-uniform distribution of the holes over the shower plate – cf. Fig. 1 – requires 3D simulation. To reduce the complexity of the computations, two sets of 2D computations were performed. In the first, the hole distribution was taken that along the radius A; in the second, along the radius B. The results of the simulations were compared to the experimental measurements, in terms of Al growth-rate profile in the radial direction of the substrate.

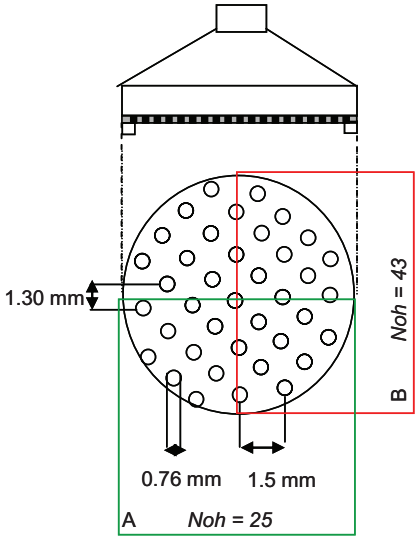

Figure 1. Schematic representation of the showerhead gas delivery system. Noh is the number of holes in the perpendicular lines A and B of the shower plate.

To calculate the growth rate of Al films, we formulate a reactive model considering homogeneous and heterogeneous chemical reactions obtained from literature (13, 14). According to these experimental observations, the Al growth rate was increased to a maximum at substrate temperature around 150^{o}C and then decreased with increasing substrate temperature (14). The activation energy of the surface reaction was found to be 9,96 kcal/mol when the substrate temperature was lower than 150^{o}C. The gas-phase reaction mechanism in Al MOCVD from DMEAA was investigated by the same research group using in situ real-time FTIR spectroscopy (13). The gas-phase dissociation reaction of DMEAA into dimethylamine (DMEA) and alane was found to be first order with activation energy of 9,56 kcal/mol. Moreover, the gas-phase DMEAA was unstable even at room temperature resulting in dissociation into DMEA and alane, and the dissociation rate was accelerated at higher gas temperatures. When the substrate temperature is higher than 150^{o}C, it is believed that alane can be readily polymerized and is not readily adsorbed on the surface to form aluminum films (5). The rapid dissociation of DMEAA in the gas phase brings about the decrease of the growth rate when the substrate temperature is above 150^{o}C. A similar effect of temperature on the growth behavior of DMEAA was also reported (15). The temperature where the maximum growth rate obtained was 160^{o}C to be compared with 150^{o}C in the work by Yun et al (14).

Taking into account all these experimental findings, the following chemical reactions considered in the reactive model of the Al growth process:

$$\left[(CH_3)_2C_2H_5\right]NAlH_3(g) \rightarrow \left[(CH_3)_2C_2H_5\right]N(g) + AlH_3(g) \quad [2]$$

$$\left[(CH_3)_2C_2H_5\right]NAlH_3(g) \rightarrow Al(s) + \left[(CH_3)_2C_2H_5\right]N(g) + 3/2\,H_2(g) \quad [3]$$

Reaction [2] occurs in the gas phase resulting in the DMEAA dissociation into DMEA and alane, while reaction [3] occurs on the surface resulting in the growth of Al films on the substrates. It is assumed that once DMEAA is dissociated in the gas phase, gas-phase alane decomposes almost immediately without contributing to the film growth (5, 16). Thus, reaction [2] is responsible for the degradation of DMEAA in the gas phase, resulting in the decrease of the growth rate at higher temperatures. Moreover, the gas-phase reaction was considered to occur only in the right direction (13). The activation energy of both reactions was obtained from the cited references (13, 14); the pre-exponential factor of the gas-phase reaction was extracted from the Arrhenius plot of the Al-N dissociation reaction rate constant (see Fig. 6 in (13)). The pre-exponential factor of the surface reaction was fitted to the experimental data.

Results and Discussion

Validation of the reactive transport model. At first, we evaluate the present reactive transport model of Al growth from DMEAA. In Fig. 2, model predictions are compared to the experimental measurements in terms of average growth rate as a function of substrate temperature. The good agreement between experimental data and simulation results, at temperatures above 200°C, fully supports the gas and surface chemistry reported in the literature (13, 14). However, a significant divergence is obtained at 160°C, where the predicted growth rate is very high compared to the experimentally measured one. This divergence can be explained by the incubation time of Al growth on silicon substrates. According to the experimental observations, the incubation time, during which

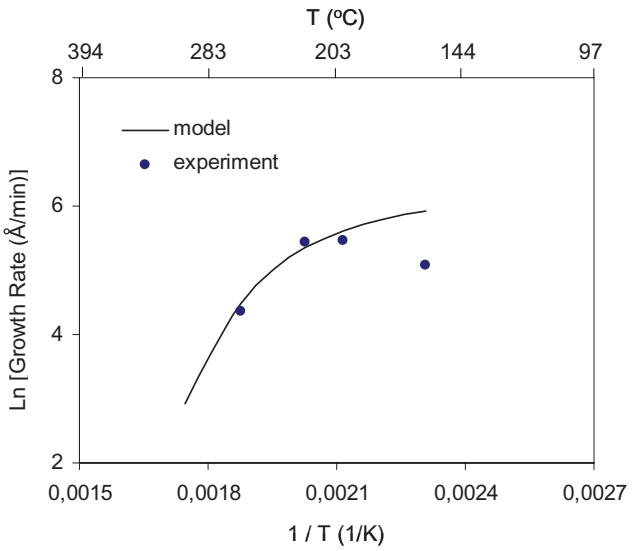

Figure 2. Arrhenius plot of Al growth rate as a function of substrate temperature. Experimental measurements versus model predictions.

no appreciable deposition had been observed at 160°C, was approximately 2 min at the centre of the substrate and almost 15 min at the edge of the substrate (i.e. at 25mm). However, the incubation time was not taken into account in the calculation of the experimental growth rates through the ratio thickness/time. The incubation time of Al growth from DMEAA has also been observed on Si and SiO_2 substrates at different temperatures (7, 15). Below 160°C, it was found that the incubation time increased from 1 to 11 min as the substrate temperature decreased (15). At 200°C, the incubation time was around 10 min (7); as temperature goes up, the incubation time becomes shorter.

Growth rate at reference conditions. In the following, the reactive transport model will be used for the thorough parametric analysis of the MOCVD reactor for Al growth. All simulations will be performed by first selecting a set of reference conditions and then by varying the value of each one of the operating parameters. The reference conditions selected in our parametric study correspond to experimental sample exp3 (see Table I). Fig. 3 depicts the predicted and measured growth rate of Al growth along the radial direction of the substrate, at reference conditions. Note that the continuous curve is the average of the model predictions at the two perpendicular radii A and B of the shower plate, which differ in the number of holes and their distribution. As shown in Fig. 3, the model predictions of the increase of Al growth in the radial direction are in good agreement with the measurements. It should be mentioned that the experimental growth rates were measured, through the weight gain of each sample, at five positions over the silicon substrate. These five samples did not belong to the same radius; thus, the experimental points represent the distribution of the growth rate over the two-dimensional substrate. On the contrary, the model predictions represent the average distribution of the growth rate over two perpendicular radii of the substrate. Taking into account the experimental error of ±8 Å/min at 220°C, the predictions of model are very satisfactory.

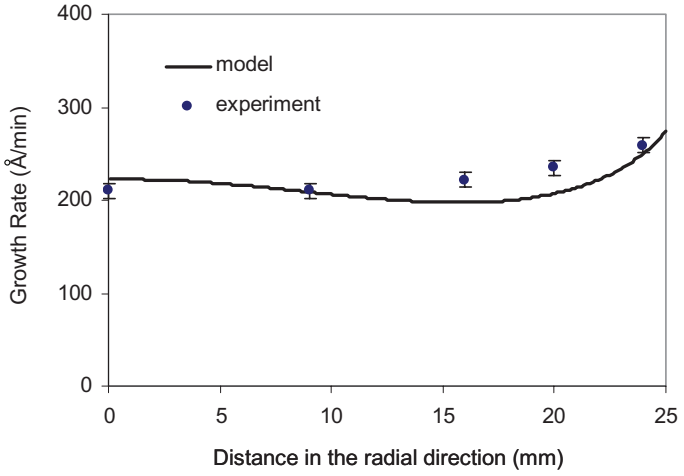

Figure 3. Al growth rate along the radial direction at reference conditions. Experimental measurements versus model predictions.

Effect of substrate temperature on film properties. Parameter continuation on the substrate temperature, T_s, is performed and growth rate profiles are calculated for temperatures from 160°C to 300°C in steps of 20°C. Note that the relative growth rate at

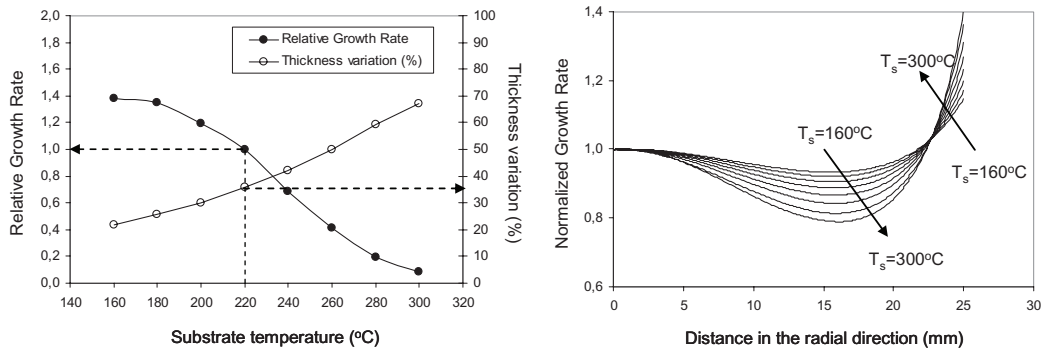

Figure 4. (a) Relative growth rate and thickness variation as a function of substrate temperature and (b) Normalized growth rate profile at different values of substrate temperature, T_s (in steps of 20^{o}C).

reference conditions (T_s = 220^{o}C) is equal to unity and that thickness variation is defined through the maximum, minimum and average growth rate, i.e. by ($GR_{max} - GR_{min}$)/ GR_{ave}. The results in Fig. 4a indicate that any increase of the substrate temperature causes a decrease of the growth rate while thickness variation increases significantly. At reference conditions, the growth rate is equal to 213,38 Å/min. Note that the decrease of the growth rate is more rapid above 220^{o}C, a consequence of the significant DMEEA degradation in the gas phase. The increased thickness variation with temperature is also shown in Fig. 4b, where the normalized growth rate profiles at different temperatures are compared. It is interesting to see from Fig. 4b that thickness variation is greater at a distance of about 16 mm from the centre of the substrate and at the edge of the substrate, i.e. at 25 mm. Moreover, there seems to be a particular distance (around 22,5 mm) where thickness variation starts increasing in the opposite direction, for all temperatures studied.

It seems that any temperature below the reference value performs much better, as it is accompanied by a greater growth rate with an improved spatial uniformity of the thickness. However, it will be recalled that the experimental growth rate at 160^{o}C is lower compared to 220^{o}C, due to the increased incubation time, as discussed previously. Therefore, a value around 200^{o}C-220^{o}C could be considered as an optimal value of substrate temperature.

Effect of reactor pressure on film properties. Parameter continuation on the reactor pressure, P, is performed and growth rate profiles are calculated for pressures in the range 5 Torr - 30 Torr, in steps of 5 Torr. The reference value of reactor pressure is 10 Torr. As shown in Fig. 5a, the increase of pressure above the reference value of 10 Torr causes a decrease of the growth rate, which approximates the value of 1,6 Å/min at 30 Torr. On the other hand, it is interesting to note the significant increase of the growth rate by a factor of 7 when pressure is decreased to the lowest value of 5 Torr. Thickness uniformity is improved at the lower pressure investigated, as also depicted in Fig. 5b. The intersection point of the curves is almost 1 mm away from the edge of the substrate. It is concluded that any lower, if feasible, value of the operating pressure, compared to the reference one, is expected to improve the properties of the Al films.

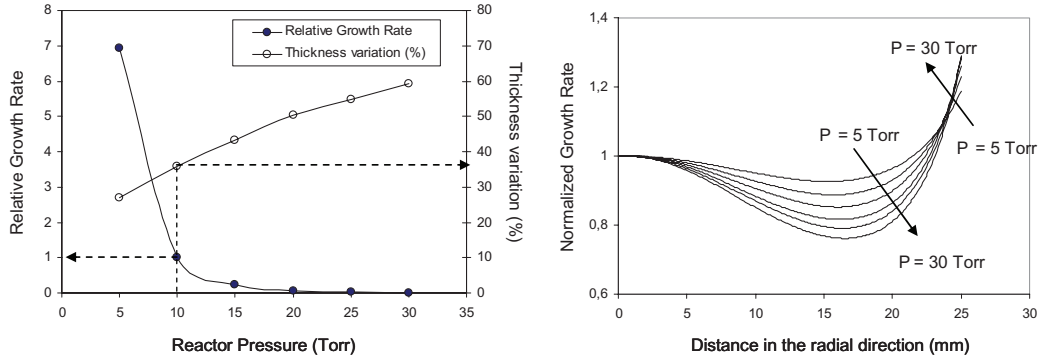

Figure 5. (a) Relative growth rate and thickness variation as a function of reactor pressure and (b) Normalized growth rate profile at different values of reactor pressure, P (in steps of 5 Torr).

Effect of dilution gas flow rate on film properties. Parameter continuation on the inlet flow rate of the dilution gas, F_d, is performed and growth rate profiles are calculated for flow rates from 105 sccm to 505 sccm in steps of 100 sccm. As shown in Fig. 6a, the reference value of F_d is 305 sccm. The results show that any increase of the flow rate of dilution nitrogen causes an increase of the growth rate. It appears that the dominant convection related to higher flow rates, and thus higher velocities, yields higher DMEAA concentrations and therefore higher growth rates. This trend in the growth rate is followed by a decrease of thickness variation, as depicted in Fig. 6b. Obviously, the increased growth rates mainly in the center of the substrate, is responsible for the improvement of the thickness uniformity at the higher flow rates.

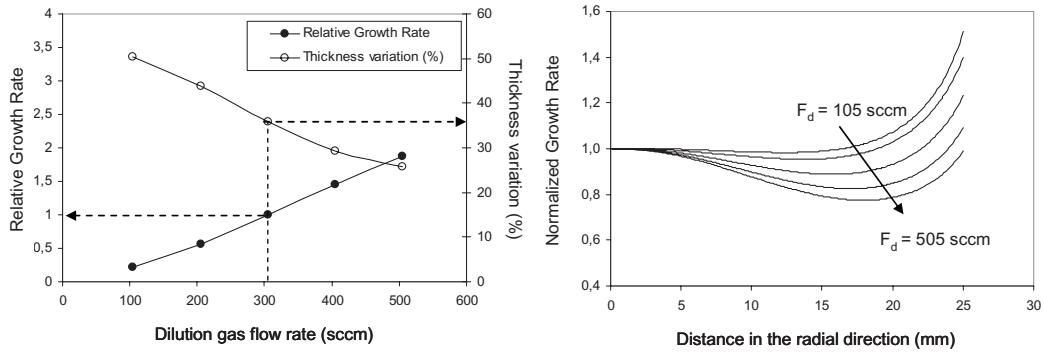

Figure 6. (a) Relative growth rate and thickness variation as a function of dilution gas flow rate and (b) Normalized growth rate profile at different values of dilution gas flow rate, F_d (in steps of 100 sccm).

Conclusions

In this work the CFD code PHOENICS has been successfully employed to solve the two-dimensional, steady state flow, heat transfer, and multi-species gas-phase and surface chemistry in an MOCVD reactor. Experimental measurements on growth-rate profiles of Al films from DMEAA at different operating conditions were used to formulate a reactive transport model, pointing out the influence of the substrate temperature. The

good agreement between model predictions and experimental data fully supports the gas and surface chemistry reported in the literature.

Simulation results indicated that growth rate and the spatial variation of the thickness depends strongly on the substrate temperature, the reactor pressure, and the inlet flow rate of the dilution gas. It is concluded that the reactive transport model can be used as a tool to guide future experimental work towards optimal parameter values and optimal shower plate designs for desired growth rates and growth shapes of Al-based complex metallic alloys.

Acknowledgments

This work was supported by the General Secretariat for Research and Technology of Greece and by the French Ministry of Foreign Affairs through the Programme for "Greece-France cooperation in Research and Technology" (contract 15207XG, 2006-2008). The support of the Agence Nationale de la Recherche in France through contract NT05-3_41834 and of the European Commission through the Network of Excellence NMP3-CT-2005-500140, are also acknowledged.

References

1. J. -M. Dubois, *Useful Quasicrystals*, World Scientific Publ. Comp., Singapore (2005).
2. C. E. C. Dam, A. P. Crzegorczyk, P. R. Hageman, R. Dorsman, C. R. Kleijn, P. K. Larsen, *J. Cryst. Growth,* **271,** 192 (2004).
3. T. C. Xenidou, A. G. Boudouvis, N. C. Markatos, D. Samélor, F. Senocq, N. PrudHomme, C. Vahlas, *Surf. Coat. Tech.*, **201,** 8868 (2007).
4. M. G. Simmonds, W. L. Gladfelter, R. Nagaraja, W. W. Szymanski, K. -H Ahn, P. H. McMurry, *J. Vac. Sci. Tecnhol. A*, **9,** 2782 (1991).
5. J. Han, K. F. Jensen, Y. Senzaki, W. L. Gladfelter, *Appl. Phys. Lett.*, **64,** 425 (1994).
6. X. Li, B. -Y. Kim, S. -W. Rhee, *Appl. Phys. Lett.*, **67**, 3426 (1995).
7. B. -Y. Kim, X. Li, S. -W. Rhee, *Appl. Phys. Lett.*, **68,** 3567 (1996).
8. M. Delmas, D. Poquillon, Y. Kihn, C. Vahlas, *Surf. Coat. Tech.*, **200,** 1413 (2005).
9. M. Delmas, C. Vahlas, *J. Electrochem. Soc.*, **154**, D538 (2007).
10. S. V. Patankar, *Numerical Heat Transfer and Fluid Flow*, Taylor & Francis, 1980.
11. CHAM Ltd., PHOENICS software, www.cham.co.uk.
12. T.C. Xenidou, A.G. Boudouvis, D.M. Tsamakis, N.C. Markatos, *J. Electrochem. Soc.*, **151**, C757 (2004).
13. J. -H. Yun, M. -Y. Park, S. -W. Rhee, *J. Vac. Sci. Technol. A*, **16**, 419 (1998).
14. J. -H. Yun, B. -Y. Kim, S. -W. Rhee, *Thin Solid Films*, **312**, 259 (1998).
15. T. W. Jang, W. Moon, J. T. Baek, B. T. Ahn, *Thin Solid Films*, **333**, 137 (1998).
16. J. W. Turley, H. W. Rinn, *Inorg. Chem.*, **8**, 18 (1969).